

Trends in rainfall regime over Israel, 1975–2010, and their relationship to large-scale variability

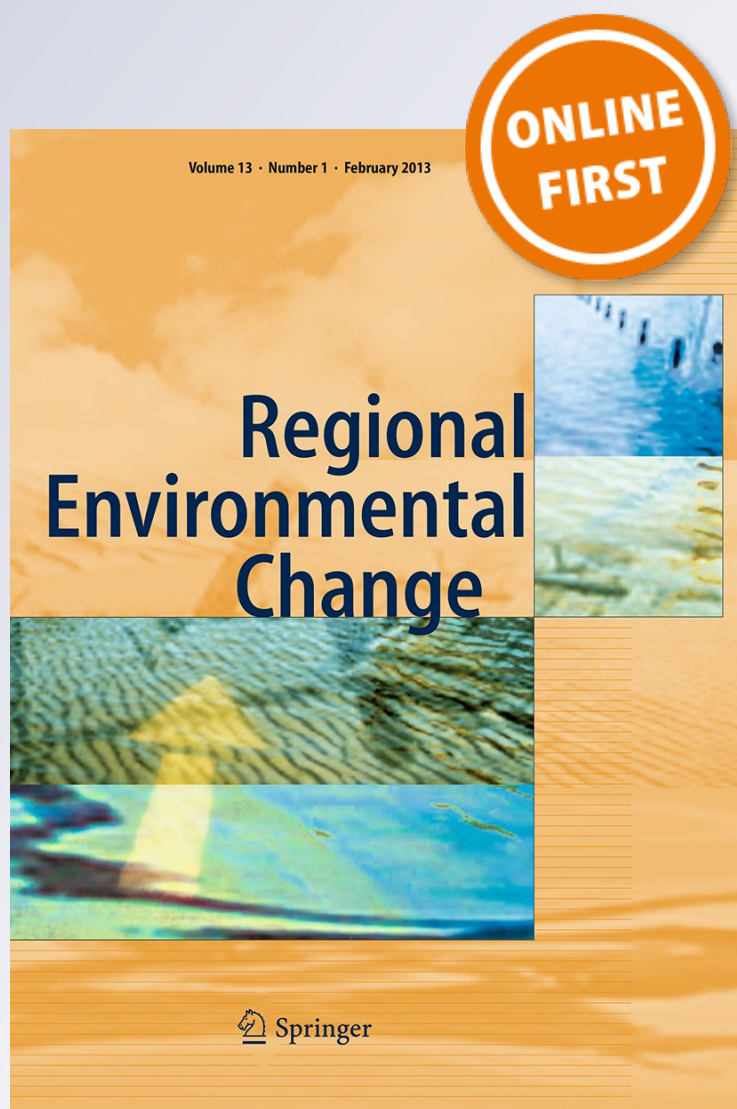
Baruch Ziv, Hadas Saaroni, Roe Pargament, Tzvi Harpaz & Pinhas Alpert

Regional Environmental Change

ISSN 1436-3798

Reg Environ Change

DOI 10.1007/s10113-013-0414-x



 Springer

Your article is protected by copyright and all rights are held exclusively by Springer-Verlag Berlin Heidelberg. This e-offprint is for personal use only and shall not be self-archived in electronic repositories. If you wish to self-archive your work, please use the accepted author's version for posting to your own website or your institution's repository. You may further deposit the accepted author's version on a funder's repository at a funder's request, provided it is not made publicly available until 12 months after publication.

Trends in rainfall regime over Israel, 1975–2010, and their relationship to large-scale variability

Baruch Ziv · Hadas Saaroni · Roe Pargament ·
Tzvi Harpaz · Pinhas Alpert

Received: 8 February 2012 / Accepted: 20 January 2013
© Springer-Verlag Berlin Heidelberg 2013

Abstract Variations and trends in the rain regime of Israel are analyzed for 1975–2010, when persistent global warming has been observed. Negative trend is observed over the majority of Israel, statistically significant only in the super-arid region. The decrease is significant over the majority of Israel only in the spring, reflecting a shortening of the rainy season, >3 days/decade. The dry spells are becoming longer, significantly in most of the stations. The factors affecting these variations, synoptic systems, large-scale oscillations and global temperature, were studied for extended period, 1953–2010. A simple multiple stepwise regression model applied for the inter-annual rainfall variations indicates that the occurrence of Cyprus lows is the dominant factor and the Mediterranean oscillation index, MOI2, is also a significant factor. In order to reduce the inter-annual noise and reveal inter-decadal variations, the time-series of the rainfall and its potential predictors were smoothed by 11-year window, showing an increase toward the 1990s, followed by a decrease, at a higher rate, onward. Correspondingly, the aridity lines propagated southward till the mid-1990s and then withdrew back, at a larger rate. The large-scale oscillations and the global temperature explain 83 % of the variance on the inter-

decadal time-scale, half of it explained by the global temperature alone. The findings of this study support the expected poleward expansion of the Hadley cell due to global warming.

Keywords Climate change · Climatic variations · Trends · Spatial and temporal variations · Cyprus low · Large-scale oscillations · Mediterranean

Introduction

Climatic models, both global and regional, are predicting a rise in temperatures and a decrease in rainfall in the Mediterranean Basin (MB), based on all scenarios of greenhouse emissions (IPCC 2007; Lionello and Giorgi 2007; Alpert et al. 2008; Kitoh et al. 2008; Jin et al. 2010; Raible et al. 2010; Krichak et al. 2011). The rainfall decrease may be the result of a poleward shift of the subtropical highs, toward the MB, as a part of the expansion of the Hadley cell due to global warming (Seidel et al. 2008). This expansion is also expressed by the predicted change in precipitation, showing bands of negative trend along the poleward sides of the subtropical highs in both hemispheres (IPCC 2007).

Decreasing trend in rainfall has far-reaching environmental implications on this sensitive region, located on the climatic border between wet (Mediterranean) and arid climates. This region is subjected to large inter-annual rainfall variability, and thus, it is difficult to identify significant long-term trends (Morin 2011). Nevertheless, a thorough analysis of rainfall variations is required in order to determine whether we can identify the predicted decreasing trend.

Most studies in recent years show a trend of rainfall decrease in the vast majority of the MB (e.g., Alpert et al.

B. Ziv · T. Harpaz
Department of Natural Science, The Open University of Israel,
43537 Ra'anana, Israel

H. Saaroni (✉) · R. Pargament · T. Harpaz
Department of Geography and the Human Environment,
Tel Aviv University, 69978 Tel Aviv, Israel
e-mail: saaroni@post.tau.ac.il

P. Alpert
Department of Geophysics, Planetary and Atmospheric Science
and the Porter School of Environmental Studies,
Tel Aviv University, 69978 Tel Aviv, Israel

2002; Xoplaki et al. 2004; Kostopoulou and Jones 2005; Toreti et al. 2010). As for the eastern MB, Alpert et al. (2002) and Zhang et al. (2005) did not identify any significant trend. For Israel, Ben-Gai et al. (1994, 1998) and Perlin and Alpert (2001) analyzed the rainfall trend between the 1960s and the mid-1990s and found an increase in the northern Negev, located at the semi-arid region of the country. They attributed this positive trend to changes in land-use due to the national water carrier, which became operational during that period, and deliver water for irrigation in large part of that region. They hypothesized that the agricultural development there led to a decrease in the surface albedo and thus to an increase in convective rains. Zangvil et al. (2003) attributed this increase in the semi-arid region to synoptic-scale factor rather than to a local one. They showed an enhanced tendency of upper-level troughs, a key factor for rainfall in Israel, to be oriented in the southwest–northeast direction, which favor rains in that part of Israel. Alpert et al. (2004) added another explanation that this rainfall increase might be from an increase in the number of days with Red Sea Trough (RST), a system having rainfall potential in south Israel.

Yosef et al. (2009) showed nonsignificant increase in the annual rainfall in Israel for the period 1951–2004, with variations in the ratio of the rainfall in the southern and the northern parts of Israel. They pointed on variations in the synoptic systems and large-scale oscillations as controlling these rainfall variations. Shlomi and Ginat (2009) examined rainfall trends in the southernmost part of Israel between the years 1950 and 2008 and indicated a significant decrease in this super-arid region.

In spite of the decrease in the total rainfall over the MB, an increase in extreme daily rainfall was found for the period 1951–1995 (Alpert et al. 2002). They showed an increase in the occurrence of torrential rain in Italy, Spain and Cyprus, and in heavy rainfall in Israel. However, these trends were statistically insignificant in Israel. Yosef et al. (2009), based on daily data from Israel for the period 1951–2004, found an increase in the relative contribution of days with >32 mm at the center and south parts of the country, and a decrease at the north. The relative contribution of days with <16 mm showed an increasing trend in the north and a decreasing trend at its center and south. However, when analyzed on a regional basis, none of these trends were statistically significant.

The rain regime in Israel is dominated by Cyprus lows (CLs, e.g., Shay-El and Alpert 1991; Goldreich 2003; Sararoni et al. 2010a). In addition, several large-scale atmospheric oscillations affect the rainfall regime (e.g., Branston and Livezey 1987; Jacobeit 1987). Price et al. (1998) showed a significant correlation between El-Nino years and rainy seasons in Israel. This connection, however, was found significant only between the mid-1970s

and the mid-1990s. The Mediterranean Index (MOI, Conté et al. 1989), the North-Sea Caspian-Sea Pattern (NCP) and the East-Atlantic–Western-Russia (EA-WR) were found to be significantly correlated with the Israeli rainfall (Kutiel and Paz 1998; Kutiel and Benaroch 2002; Krichak et al. 2002). Yosef et al. (2009) indicated that inter-annual rainfall variations are significantly correlated with both the EA-WR and the NCP oscillations.

Several studies indicated that the North Atlantic Oscillation (NAO) is not correlated with the rainfall in Israel (e.g., Ziv et al. 2006). However, Zangvil et al. (2003) claimed that the positive phase of the NAO (between the mid-1970s and the mid-1990s) is the cause for the aforementioned unique orientation of the upper troughs, responsible for the rainfall increase in the semi-arid region of Israel. Krichak et al. (2002) and Krichak and Alpert (2005) found a combined effect of the NAO and the EA-WR on the rain regime in Israel.

The aim of this research is to examine variations and trends in the rain regime over Israel with respect to variations in the occurrence of the synoptic systems, the large-scale oscillations and the global temperature. Our goal is to find whether the expected drying trend, implied by the future projections of the climate models, can be already identified during the period of consistent rise in the global temperature (IPCC 2007), that is, from the mid-1970s.

Materials and methods

Data

The study area covers the entire area of Israel, with annual rainfall ranging from 25 mm in the southernmost tip to >1000 mm in the northern mountains (Fig. 1a). The study area was divided according to the geographical and climatological features (geographical regions, hereafter), as defined by the Israel Meteorological Service (IMS, Fig. 1b). The rain data were inspected by the climate department of the IMS, and no homogenization was needed. However, fitting data from neighboring stations (in the range of ~ 10 km) was done when needed.

Monthly rainfall data are based on all available rain-measuring stations of the IMS, that is, 919 stations (denoted in Fig. 1a). Daily data from 10 representing stations (denoted in Fig. 1b) are analyzed for exploring trends in the structure of the rainy season (as specified in the methods section). The data of these stations are full, except for one station (Sedom, at the super-arid region of the Dead Sea), where two seasons were missing and accomplished by the IMS, based on neighboring stations.

Since the rain in Israel is obtained in the months October–May (Goldreich 2003), the rain season is defined as starting

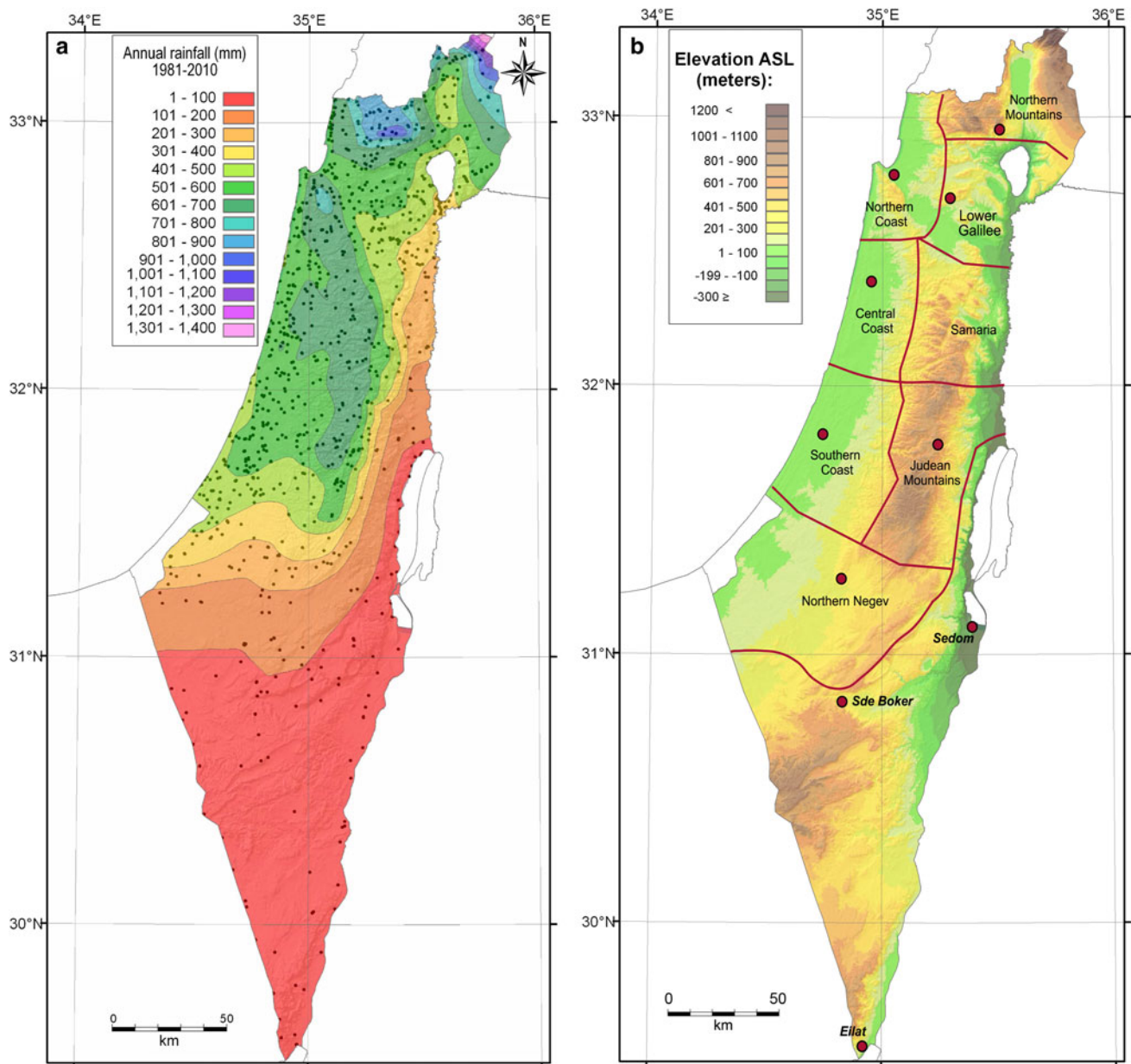


Fig. 1 **a** Average annual rainfall in Israel (1981–2010) with notation of all the stations (919) used in the study. **b** The geographical regions and the location of the 10 “representative stations”

at August 1 and ending at the next July 31. The study period includes 36 rain seasons, between the years 1974/5 and 2009/10, during which the global temperature is rising persistently (IPCC 2007). For inter-decadal analysis we refer also to a longer period, that is, 1952/3–2009/10 (extended period, hereafter), for which the data available are the annual rainfall averaged over the region with >100 mm.

Methods

Linear trends in the annual rainfall, number of rain days, daily rainfall intensity, length of the rain and dry spells and

the timing and duration of the rainy season were derived using both the least-squares regression, with the Pearson's correlation coefficient for evaluating their statistical significance, and the non-parametric method of Mann–Kendall (Helsel and Hirsch 2002). The two-tailed p value is considered since there was no a-priori expected trend for any of the variables. The rain spells are derived for the entire rainy season, October–May, and the dry spells, for the period November–March, so that the long dry spells characterizing the beginning or the end of the rainy season are discarded. The duration of the rainy season is determined based on the method of Paz and Kutiel (2003),

applied for the MB by Reiser and Kutiel (2009). The beginning of the rainy season is defined as the date by which 10 % of the annual rainfall for the pertinent year is accumulated and its end as the date by which 90 % of the annual rainfall is accumulated. The advantage of this method is that it ignores sporadic rain events at the beginning and the end of the rainy season.

The long-term trend of the annual rainfall (using the least-squares regression method) over the area with >100 mm was mapped using the ArcGIS 9.3 software (ESRI 2008) and the interpolation method of Inverse Distance Weighted (IDW). In order to better assess the data in regions with a sharp rainfall gradients, the interpolation was done on the annual rain anomaly values rather than the rainfall itself, so that the values of the individual stations were interpolated into a 3×3 km grid. The mapping does not include the super-arid region at the southernmost part of Israel and the Dead Sea areas due to the large variability characterizing this area and the insufficient amount of rain gauges there. In addition, the trend, together with its statistical significance, is calculated for each of the geographical regions (see Fig. 1b) separately.

One of the implications of changes in the annual rainfall, most relevant to the study region, is a shift in the location of the climatic borders. Based on Köppen classification (McKnight and Hess 2008), the climatic borders between the Mediterranean and the semi-arid and between the semi-arid and arid regions for the study region, characterized by winter rainfall and an average annual temperature of 20 °C, coincide with the 400 mm and the 200 mm isohyets, respectively. The inter-annual variations in the location of these isohyets and in the area included in each of the climatic regions are analyzed based on all stations located in the relevant region (see Fig. 1a).

The relationships between the annual rainfall and factors that may explain its inter-annual and inter-decadal variations are studied for the extended period. This includes the occurrence of the regional synoptic systems, the large-scale oscillations known to affect the MB and the global temperature. The definition of the regional synoptic systems is based on the semi-objective synoptic classification of Alpert et al. (2004), including five systems that are further divided into 19 types. This classification is based on the 12 UTC 1000-hPa temperature, horizontal wind and geopotential height, reflecting the surface pressure systems. The rain-producing systems considered here are the CL, being the major rain-producing system, and the RST, known as a source of flash floods in south Israel (Kahana et al. 2002). It should be stressed that the occurrence of a synoptic system refers to the number of days in which it appeared in the synoptic maps of the eastern MB. For instance, an individual CL that persisted 3 days near Cyprus would be counted three times. The large-scale oscillations analyzed

are the NAO, EA-WR, NCP, Nino3.4 and MOI2 (the 500-hPa geopotential difference between Gibraltar and Beit Dagan, Israel), taken from NOAA-CIRES, Climate Indices: Monthly Atmospheric and Ocean Time-Series (<http://www.esrl.noaa.gov/psd/data/climateindices/>). The global temperatures, in terms of anomaly with respect to the 1951–1980 average, were taken from the National Aeronautics and Space Administration, Goddard Institute for Space Studies (<http://www.esrl.noaa.gov/psd/data/correlation/gmsst.data>).

The relationships between the rainfall and the aforementioned factors were first examined by correlating its annual amounts with the occurrence of the synoptic systems, the indices representing the large-scale oscillation and the global temperature anomaly. Then, a simple multiple stepwise regression model (regression model, hereafter) was applied (e.g., Sousa et al. 2011), using the SPSS software applying the forward stepwise option. The regression model aims to identify the significant factors explaining the inter-annual and inter-decadal variations in the rainfall and to reconstruct the annual rainfall (predictant) based on a linear combination of factors (potential predictors). The regression model was calibrated and validated by the standard cross-validation technique of “leave one out” (Wilks 2011). This technique is based on repetitive derivations (runs) of the regression model. In each run one data point (i.e., one year) is excluded (left out), the model parameters are determined based on the remaining data points, and the model is applied on the left-out data point. N runs are performed (N is the number of data points, i.e., years), so that in each one, another data point is left out. For each run the error in the regression model of the left-out point and the parameters are saved. The model errors in the individual runs were used for calculating the model's standard error.

The skill of the regression model was evaluated using the SS factor (Wilks 2011), given by $(1) SS = 100 \times \frac{RMSE - RMSE_{ref}}{RMSE_{perf} - RMSE_{ref}}$, where $RMSE_{ref}$ is the standard error of an alternative reference prediction scheme and $RMSE_{perf}$ is the standard error of a perfect prediction. If $SS = 0$, the skill of the regression model is similar to that of the reference prediction. If $SS = +100$, the prediction skill reaches the quality of the perfect prediction, and if $SS = -100$, the prediction is much worse than the reference one. Reference prediction models commonly used for the seasonal value of a climatological variable are its climatological long-term mean (“climatology”) or its value in the previous year (“persistence”), see Sousa et al. (2011).

Regression model was applied also on smoothed time-series (using 11-year running average) of the rainfall and the aforementioned factors for exploring relationships on the decadal time-scale. The inter-decadal analysis was redone, for the detrended time-series.

Observed trends

Variations and trends in the annual rainfall and the aridity lines

The average annual rainfall in the region with >100 mm for the study period (1974/5–2009/10) is 429 mm, with a standard deviation of 116 mm, that is, an inter-annual variations of over 25 %. The inter-annual variation and the long-term trend of the annual rainfall averaged over this region are presented in Fig. 2. The implied linear trend for the study period is a decrease of -2.7 and -1.9 % per decade according to the least-squares regression and the Mann–Kendall methods, respectively. This trend is not statistically significant by both methods. The inter-decadal variation, reflected by a polynomial curve (3rd order, Fig. 2), is characterized by a slight increase at the beginning of the study period, followed by a decrease, in a larger rate toward the end of the study period. It could be hypothesized that this course results from the unusual rainy season of 1991/92. However, when this exceptional rainy season was removed from the time-series, the polynomial course remained almost similar. The average annual rainfall for this region for the extended period (beginning at 1952/3) shows also a negative linear trend, though being considerably smaller, -0.1 and -0.5 % per decade, according to the two methods (not shown). These results demonstrate fluctuations in the annual rainfall on the decadal time-scale rather than a consistent decreasing trend.

The spatial distribution of the linear trend for the study period (Fig. 3a) shows a decrease over most of the region, though being statistically insignificant over the vast majority of the area. The largest decrease is found in the Northern Mountains and the Judean Mountains. In certain locations a slight increase is observed, especially in the center of Israel. The linear trend averaged over each of the geographical regions, using both of the aforementioned methods, is presented in Fig. 3b. It further indicates the

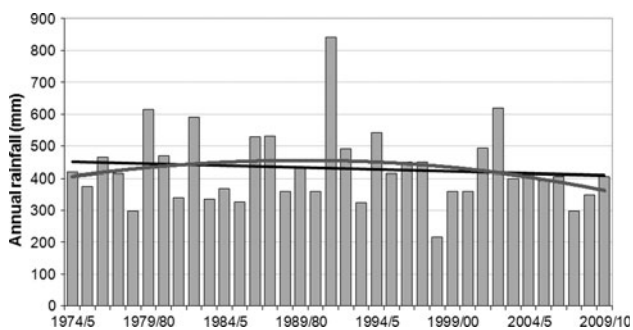


Fig. 2 Inter-annual variations of the annual rainfall averaged over the region with >100 mm, together with the linear trend (*black*) and the polynomial curve (third-order, *gray solid*) for the study period (1975–2010)

general decreasing trend (still statistically insignificant), even in regions in which local increase is noted (see Fig. 3a). In the super-arid region, a larger decrease is found, exceeding -25 %, in the southernmost point, Eilat, being statistically significant. These results go in line with Shlomi and Ginat (2009), who found a significant decrease in the southern, super-arid, part of Israel for the period 1950–2008.

A major aspect of changes in the annual rainfall is a shift in the location of the borders of the climatic regions, the wet (Mediterranean), semi-arid and arid regions. The inter-annual variability in their location is exemplified by that of the 200 mm isohyet (representing the border between the semi-arid and the arid regions) for each year along the study period (Fig. 4). For example, the most northward transition of this isohyet, ~ 50 km into the wet (Mediterranean) region, occurred in the extreme dry year of 1998/9. The inter-annual variations in the relative area of each of the three climatic regions, shown in Fig. 5, reflect a shrinking of the wet region, at a rate of 2.5 %/decade (statistically insignificant), versus an increase in the area of both the semi-arid and the arid regions. The location of the aridity lines (200 and 400 mm) was averaged for three consecutive 12-year sub-periods (not shown). This analysis indicates that both lines propagated southward, toward the arid region, between the first and the second sub-periods, and withdrew back at a larger rate, toward the wet region, between the second and the third sub-periods. This is consistent with the rainfall increase toward the 1990s and the decrease, in a larger rate, toward the end of the study period (see Fig. 2).

Trends in other features of the rainfall regime

This section addresses changes in the daily rainfall, in the course of the rainy season and in the duration of the rain spells and the dry spells separating between them. The average trend in the daily rainfall was derived by dividing the trend of the annual rainfall by that of the number of rain days. The number of rain days is found to decrease in the majority of the stations located in the wet and the semi-arid parts of Israel, as the rainfall does, but in a larger rate, implying that the average daily rainfall is increasing (though statistically insignificant). The trends in the relative portion of days with >30 mm and >50 mm (heavy rainy days) out of the total rain days were also examined. No consistent trend is found, including among neighboring stations belonging to the same geographical region. It is worth noting that in the coastal plain, the percentage of heavy rainy days was found to increase during the study period (also statistically insignificant).

Trends in the course of the rainy season have also vast environmental implications, such as changes in the

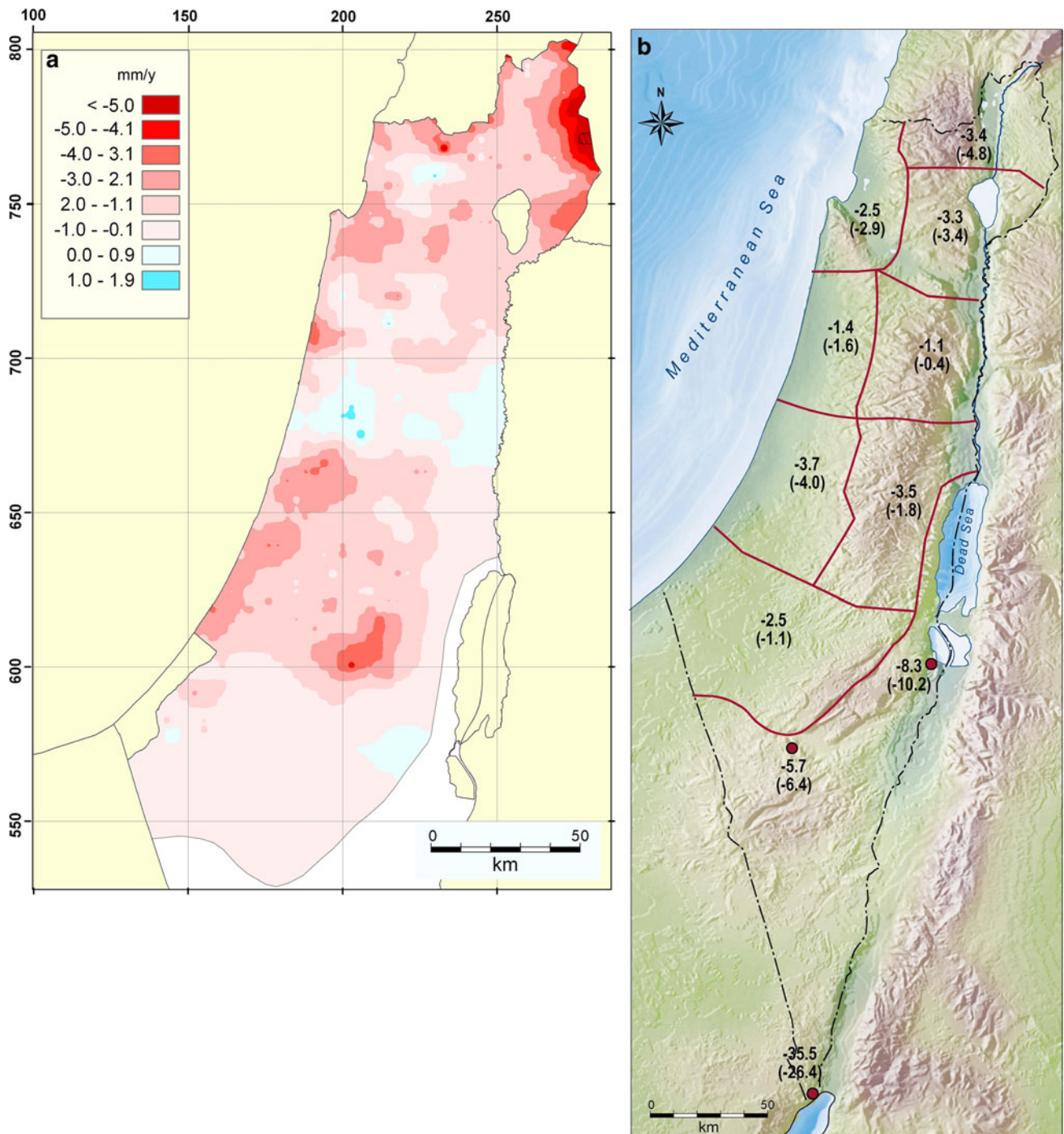


Fig. 3 **a** Spatial distribution of the long-term trend, mm/y, for the study period (1975–2010), based on the least-square regression, over the region with annual average rainfall of >100 mm. The black line encircles the area in which the trend is statistically significant

according to Pearson correlation. **b** The average long-term trend, %/decade, in each of the geographical regions, according to the least-square regression and to the Mann-Kendall method (in parenthesis)

duration of the agricultural growing season and various hydrological aspects. The distribution of the monthly rainfall (averaged over the region with >100 mm) for two 20-year sub-periods, 1974/75–1993/94 and 1990/91–2009/10, indicates a narrowing of the curve, suggesting a shortening of the rainy season, most pronounced in the

spring, mainly in March. However, since the difference in the monthly rainfall between the two sub-periods for each month is several times smaller than the standard deviation, these results are statistically insignificant. Changes in the course of the rainy season were further explored by calculating the linear trend of the rainfall for each part of the

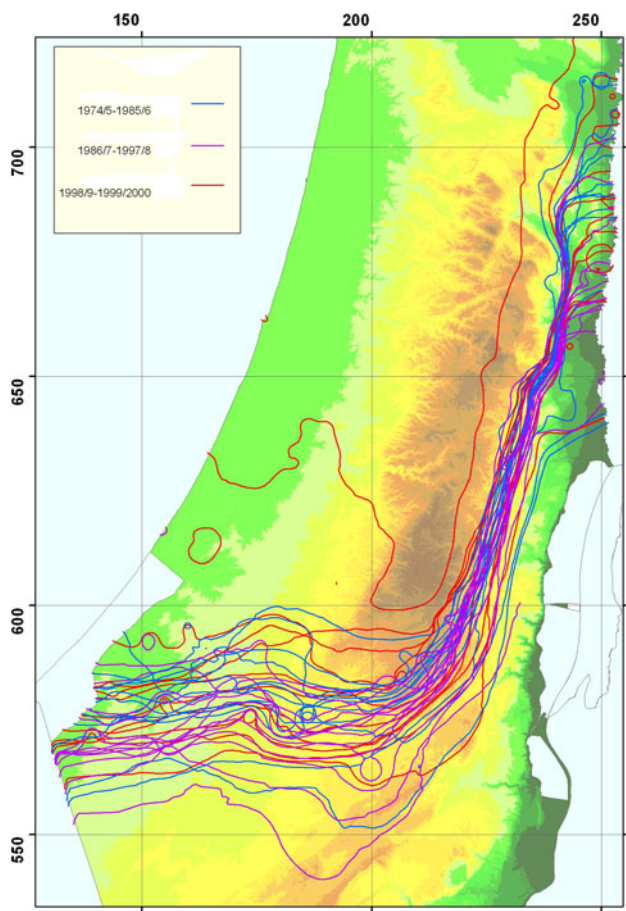


Fig. 4 The location of the 200 mm isohyet (representing the border of the arid region) for the individual years included in the study period (1975–2010)

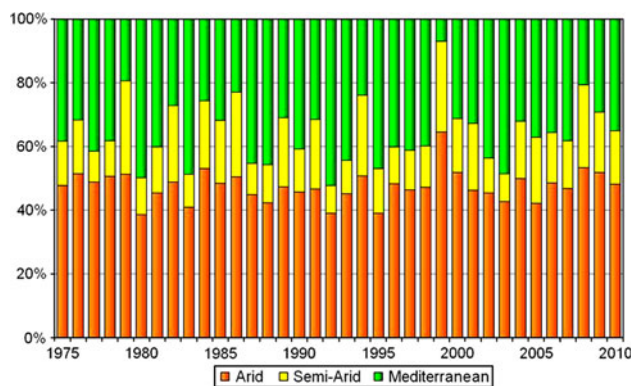


Fig. 5 Inter-annual variations in the percentage of the arid (<200 mm, orange), semi-arid (200–400 mm, yellow) and the Mediterranean (>400 mm, green) climatic regions along the study period (color figure online)

season: autumn (September–November), winter (December–February) and spring (March–May). Only in the spring a significant decrease is found, at a rate of >15 %/decade according to the two methods, both statistically significant.

Trends in the duration of the rainy season were examined based on the time that passes between the

accumulation of 10 and 90 % of the annual rainfall, following Reiser and Kutiel (2009). These trends are exemplified by two stations, Haifa and Jerusalem (Fig. 6a, b), representing the northern coastal region and the central (Judean) Mountains of Israel, respectively. The vertical axis in Fig. 6 denotes the serial day of the rainy season starting at October 1. The red and blue straight solid lines show the linear trends in the beginning (10 %) and the ending (90 %) dates of the rainy season, respectively. The interval between them (~110 days in both stations) reflects the duration of the rainy season. The trend of the beginning time of the rainy season is positive in both stations, while that of its ending is negative, indicating a shortening of the rainy season from both sides. The average shortening rate is ~3 %/decade (statistically insignificant), mostly due to the anticipation of the season ending. Similar trends were found for all representative stations, except one (in the Dead Sea, see below), all statistically insignificant, presumably due to the large inter-annual variations (well seen in Fig. 6). The opposite trend found in the super-arid area of the Dead Sea may be attributed to extreme rain events that occurred near the ends of several rainy seasons at the latest decade, that is, May 2001, October 2004 and May 2007.

Trends in the duration of the rain and dry spells within the rainy season have also important environmental implications, especially for agriculture and ecosystems. For instance, long dry spells may cause drying of the soil, implying that more irrigation is needed, whereas longer rain spells may increase flooding risk. Inter-annual variations and the trend in the duration of the rain and dry spells were analyzed (Table 1). Regarding the rain spells, no consistent or statistically significant trend was found. As for the dry spells, a lengthening trend was found in all representative stations, being statistically significant, in six out of the 10 stations analyzed, at the 90 % level, and in four of them, at the 95 % level (see Table 1). The average duration of dry spells for the stations located at the region with >200 mm is 5.2 days. This duration was found to lengthen at an average rate of 1.1 days during the study period, that is, 6.1 %/decade (statistically significant at the 95 % level).

External factors controlling the rainfall variations

External factors that can explain the inter-annual variations in the rainfall are the occurrence of the relevant synoptic systems, the large-scale oscillations and, potentially, the global temperature. On the inter-decadal time-scale, the rainfall variations resulting from synoptic and large-scale factors may mask the long-term linear trend. The first subsection analyzes the relationships between the inter-annual

Fig. 6 Inter-annual variations in the dates by which 10 % (red) and 90 % (blue) of the seasonal rainfall are accumulated and the linear trend, according to the least-square regression, for two stations representing the northern coastal plain (Haifa, a) and the central mountains (Jerusalem, b) along the study period. In the y axis, 0 corresponds to October 1, 60 corresponds to November 29, 160 corresponds to March 9, etc (color figure online)

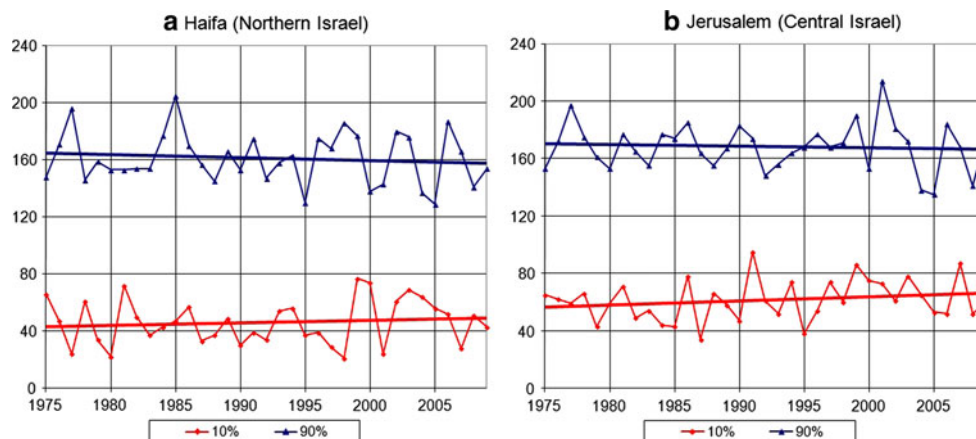


Table 1 Average duration (number of days) and linear trend (%/decade), calculated according to the least-square regression and to the Mann–Kendall method (in parenthesis), of the rain spells (October–May) and the dry spells (November–March) for the representative stations in the geographical regions of Israel

Region	North Mountains	North Coast	Lower Galilee	Central Coast	South Coast	Judean& Samaria	North Negev	Sede Boqer	Sedom	Eilat
Rain spell average duration (\pm STD, days)	2.8 \pm 2.2	2.5 \pm 1.9	2.5 \pm 1.9	2.4 \pm 1.7	2.3 \pm 1.6	2.4 \pm 1.7	2.0 \pm 1.2	1.7 \pm 1.0	1.4 \pm 0.7	1.4 \pm 0.9
Trend (%/decade)	-1.2 (-1.6)	-1.2 (-0.9)	-1.9 (-2.4)	-2.1 (-0.9)	+0.0 (+0.1)	-0.8 (-0.8)	+1.3 (+2.3)	<u>-4.1</u> (-4.6)	+0.6 (+0.0)	-10.7 (-6.9)
Dry spell average duration (\pm STD, days)	4.3 \pm 3.9	4.8 \pm 4.3	4.8 \pm 4.3	4.9 \pm 4.4	5.4 \pm 5.1	4.9 \pm 4.6	6.1 \pm 5.6	8.5 \pm 8.4	13.8 \pm 14.0	17.4 \pm 19.2
Trend (%/decade)	+7.0 (+6.3)	+7.4 (+6.9)	+9.6 (+10.4)	<u>+6.2</u> (+5.6)	+3.7 (+4.7)	<u>+6.3</u> (+6.6)	+4.0 (+5.2)	<u>+27.3</u> (+3.6)	+2.5 (+0.9)	+50.7 (+22.0)

Values significant at the 95 % level (two-tailed) are bold, and those significant at the 90 % level are underlined

variations in these factors and the annual rainfall, and the second, with the inter-decadal variations, attempts to isolate the contribution of the global warming. Both analyses are done for the extended period, that is, 1952/3–2009/10.

Inter-annual variations

The linkage between the annual rainfall and the synoptic systems was first analyzed by correlating its inter-annual variation with that in the occurrence of the CLs and the RST. The correlation was calculated for the average rainfall of each of the geographical regions, based on all stations, and for the three super-arid stations. The most correlated factor for north and central Israel is the annual occurrence of CLs ($R > +0.7$). The correlation decreases southward, down to +0.49 in the northern Negev, and vanishes in the super-arid region (Table 2). This demonstrates the role of the CL as the main rain-producing system

and as the controller of the inter-annual rainfall variations, even in the semi-arid region located >600 km away from the CLs track (Alpert et al. 1990), in agreement with Saaroni et al. (2010a).

As for the RST, a negative correlation (statistically insignificant) was found for most of the geographical regions, including the super-arid stations, suggesting that the RST is essentially a system that prevents rain. This finding disagrees with studies analyzing severe rain events in south Israel, associated with “active” RST (e.g., Kahana et al. 2002). The apparent contradiction can be settled by the fact that the majority of days in which the RST prevails over the region are inactive (e.g., Tsvieli and Zangvil 2005). This is due to upper-level ridges that commonly accompany the lower-level RST that prevents rain formation (e.g., Saaroni et al. 2010b).

The rainfall was also correlated with the large-scale oscillations, including the Nino3.4, EA-WR, NCP, MOI2

Table 2 Correlations between the yearly rainfall and the synoptic and large-scale oscillations for the geographical regions and the three stations located at the super-arid region

Study period	Geographical region/ station	Annual rainfall (± STD), mm	Correlation (<i>R</i>) with the annual rainfall					
			Cyprus low (CL) days	Red Sea Trough (RST) days	Nino 3.4	EA-WR	NCP	MOI2
1975–2010	Northern Mountains	694 (±186)	+0.71	−0.15	+0.60	+0.34	+0.33	+0.47
	Northern Coast	632 (±158)	+0.73	−0.08	+0.59	<u>+0.29</u>	+0.29	+0.52
	Lower Galilee	478 (±136)	+0.72	−0.11	+0.58	+0.33	+0.37	+0.50
	Central Coast	591 (±167)	+0.77	−0.06	+0.59	<u>+0.28</u>	<u>+0.31</u>	+0.58
	Samaria	466 (±138)	+0.71	−0.06	+0.62	<u>+0.32</u>	+0.41	+0.60
	Southern Coast	478 (±150)	+0.72	−0.06	+0.59	+0.39	+0.40	+0.66
	Judean Mountains	360 (±108)	+0.64	−0.06	+0.62	+0.34	+0.37	+0.61
	Northern Negev	174 (±53)	+0.49	+0.05	+0.61	<u>+0.29</u>	+0.23	+0.62
	Sede Boqer	93 (±39)	<u>+0.29</u>	−0.12	+0.41	+0.19	+0.09	+0.36
	Sedom	41 (±24)	+0.06	−0.07	+0.08	+0.12	−0.10	+0.04
	Eilat	23 (±18)	−0.01	−0.22	+0.03	−0.07	<u>−0.31</u>	−0.05
	>100 mm	429 (±116)	+0.74	−0.07	+0.64	+0.35	+0.37	+0.61
1953–2010	>100 mm	414* (±105)	+0.68	−0.11	+0.33	+0.31	+0.32	+0.50

Values significant at the 95 % level (two-tailed) are bold, and those significant at the 90 % level are underlined

* The lower average rainfall for the extended period stems from the absence of data for the Golan Mountains (part of the Northern Mountains) up till the early 1970s, and thus, this rainy area is not included in the extended period database

and the NAO (Table 2). All of them, except the NAO, were found significantly correlated with the annual rainfall in most of the geographical regions, in agreement with previous studies (Price et al. 1998; Kutiel and Benaroch 2002; Krichak and Alpert 2005; Ziv et al. 2006). The correlations with the Nino3.4 and the MOI2 were the highest, around +0.6 over the wet and semi-arid parts of Israel. No significant correlation was found with the NAO and the global temperature for any of the geographical regions (thus not included in Table 2). The correlation between the annual rainfall in the super-arid region and both synoptic- and large-scale factors was found poor, indicating that the rain regime there is dominated by local effects and convective systems (as shown, e.g., by Dayan and Sharon 1980; Dayan et al. 2001; Kahana et al. 2002). Therefore, the linkage between the external factors and the annual rainfall is analyzed hereafter for the region with >100 mm.

The correlation between the annual rainfall (averaged over the region with >100 mm) and the CL occurrence is significantly high, +0.74 and +0.68 for the study period (1974/5–2009/10) and the extended period (1952/3–2009/10), respectively. As for the MOI2, NCP and EA-WR oscillations, the correlations were also statistically significant, that is, $R > +0.3$ (the significance threshold for a 35-year period), for both the study period and the extended period (see Table 2). The correlation with the Nino3.4 for the extended period ($R = +0.33$) is considerably lower

than that for the study period ($R = +0.64$), in agreement with Price et al. (1998). No correlation was found with the NAO also for the extended period.

The significant correlation found between the annual rainfall and both the CL occurrence and large-scale oscillations suggests that the occurrence of the CLs and the large-scale oscillations are correlated between them. In other words, the annual rainfall may be controlled by the large-scale oscillations both directly, and indirectly via the CLs. Analysis done for the extended period shows that three oscillations, MOI2, EA-WR and NCP, are significantly correlated with the CL occurrence (Fig. 7). These oscillations are also highly correlated with the annual rainfall itself (Table 2), except the Nino3.4, which is not correlated with the CL occurrence, but is significantly correlated with the annual rainfall.

In order to quantify the contribution of the major external factors, a regression model (see “methods” section) was derived for the annual rainfall, averaged over the region with >100 mm (the predictant). The potential predictors are the occurrence of the relevant synoptic systems (CLs and RST), the five large-scale oscillations and the global temperature. The regression model, applied for the extended period, yielded two significant predictors, the CL occurrence and the MOI2. The standard error of this regression model, derived by the standard “leave one out” cross-validation, is 77.1 mm, that is, 19 % of the average annual rainfall and 73 % of its STD. The correlation

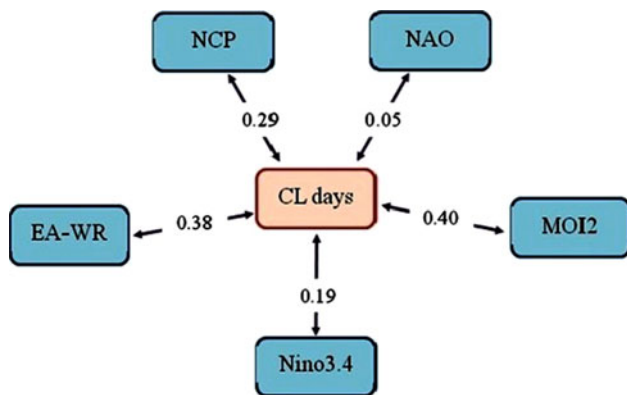


Fig. 7 Correlations between the large-scale oscillations and the number of CL days, based on data for the extended period (1952/3–2009/10)

between the predicted and the actual rainfall is $R = +0.73$, implying that these two predictors explain 53 % of the inter-annual rainfall variation.

The skill of the regression model was evaluated using the *SS* factor (see “methods”). When “climatology” was applied as a reference prediction model, the standard error obtained was 105.3 mm, and when “persistence” was used as a reference prediction model, it yielded a standard error of 159.3 mm. The larger standard error obtained for the “persistence” reference prediction model over the “climatology” can be explained by the weak correlation ($R = -0.12$, statistically insignificant) found between the rainfall time-series and that of the previous year (one year lag). The *SS* was calculated, applying for $RMSE_{ref}$, the standard errors of the two aforementioned reference prediction models. We applied for $RMSE_{perf}$ 41.4 mm (10 % of the average annual rainfall), since this interval is considered as acceptable in seasonal forecast of annual rainfall in Israel (by the IMS). The resulting *SS* are +70 and +44 when the standard errors of the “climatology” and “persistence” models, respectively, were used as $RMSE_{ref}$. This implies that our regression model is considerably more accurate than those based on “climatology” or “persistence”.

Inter-decadal variations

The variation of the annual rainfall (averaged over the region with >100 mm) and the polynomial curve (6th order) for the extended period (Fig. 8a) show prominent inter-decadal variations, that is, a maximum in the 1990s and a decrease since the late 1990s onward (as seen also in Fig. 2). A similar course is seen in the curve based on 11-year smoothed time-series (Fig. 8b, thick green line), except for the decrease at the beginning of the extended period (seen in Fig. 8a) which cannot be included in the smoothed time-series.

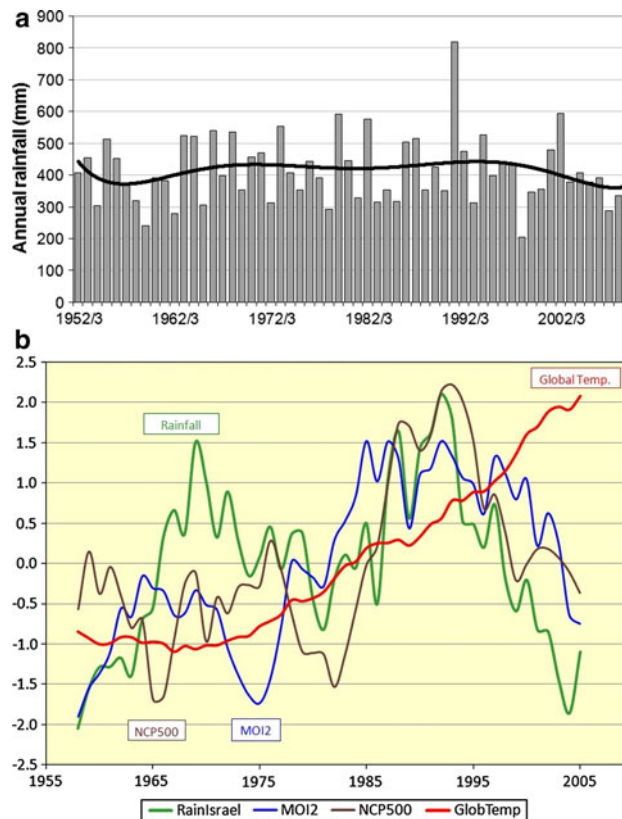


Fig. 8 a Inter-annual variation of the annual rainfall averaged over the region with >100 mm, together with the polynomial (6th order) curve (thick solid line) for the extended period (1953–2010). **b** Inter-annual variations in the 11-y running average of the annual rainfall (green), the MOI2 (blue), the NCP (brown) and the global temperature (red). All of the graphs are normalized and standardized (color figure online)

In order to identify factors explaining these variations, the time-series of the rainfall, the CL occurrence, the large-scale oscillations and the global temperature were smoothed, using running average with varying time-window, from 5 to 13 years. The correlation between each of these factors and the rainfall (as a function of the smoothing time-window) is shown in Table 3, indicating that the CL occurrence remains the dominant. As for the large-scale oscillations, all of them, except the NAO, show significant correlation with the unsmoothed time-series (see Table 2 and previous section). When two significantly correlated series are smoothed, one would expect that the correlation between them would increase (positive tendency). Here, this positive tendency is most pronounced for the NAO ($R = +0.08$ for the unsmoothed time-series and $R = +0.48$, significant at the 95 % level, for the 13-year smoothing) and for the NCP (see Table 3). While for the inter-annual variations in the rainfall, the MOI2 is clearly the most correlated large-scale oscillation (see Table 2), for the decadal time-scale the order of significance is changed, that is, the NCP is the most significant oscillation

Table 3 Correlations between the rainfall and the external factors as a function of the smoothing time-window

Factor/Smoothing time-window	Cyprus low (CL) occurrence	NAO	Nino3.4	EA-WR	NCP	MOI2	Glob temp.
None	0.68	0.08	0.33	0.31	0.32	0.50	-0.01
5 years	0.82	0.31	0.40	0.35	0.35	0.39	-0.09
9 years	0.87	0.38	0.43	0.29	0.46	0.45	-0.01
11 years	0.84	0.43	0.40	0.26	0.49	0.49	-0.06
13 years	0.83	0.48	0.37	0.27	0.55	0.48	-0.04

Correlations statistically significant at the 95 % level (two-tailed) are bold

(for the 13-year smoothing), followed by the MOI2 and the NAO. The global temperature, however, remained uncorrelated with the rainfall along the smoothing process.

The course of the annual rainfall, the MOI2, the NCP and the global temperature, smoothed to the decadal scale (11-year time-window) is shown in Fig. 8b. The rainfall curve (green) reflects a course most similar to that seen in the polynomial approximation shown in Fig. 8a. The two extrema, one toward the end of the 1960s and second, most pronounced, in the early mid-1990s, are in-phase with the NCP and the MOI2 (as well as with the other three large-scale oscillations, not shown), being in their maximum in the 1990s and in their minimum in the following decade. Note that the rainfall curve in the late 1960s and the 1970s (in Fig. 8b) is above those of the NCP and the MOI2 and decreases gradually below them from the late 1980s, toward the end of the study period. This raises the need to analyze the quantified contribution of each of the proposed factors assumed to be relevant to the decadal time-scale.

Accordingly, the regression model was applied for the 11-year smoothed time-series and for detrended time-series. As a first step, the list of potential predictors included the CL occurrence, the five large-scale oscillations and the global temperature. At the second step, the CL occurrence was removed, in order to assess the contribution of the external factors, that is, the large-scale oscillations and the global temperature. In order to estimate the contribution of the global temperature, in the third step, the regression model was applied while excluding the global temperature

and the CL occurrence from the set of potential predictors. While comparing the results of steps #2 and #3, the contribution of the global temperature is revealed. The significant predictors and the variance explained (R^2) in each of the six runs (11-year smoothed time-series and the same for these time-series, in which each of the variables was detrended separately) are specified in Table 4. In addition, the regression models were evaluated by the SS factor, based on the “leave one out” validation and “climatology” as a reference model. The standard error of the perfect prediction model (see previous section) was divided by $\sqrt{11}$ (so that $RMSE_{perf}$ was 12.5 mm), since the data were smoothed by 11-year running average.

The hierarchy of the natural variance explained by the significant predictors and the SS factor found among the three combinations of potential predictors was similar for the original and the detrended time-series. The SS for the original smoothed data including all factors was +62. When the CL occurrence was excluded, it dropped to +33, and when the global temperature was also excluded, it further dropped to +12. The respective values for the detrended data were higher, that is, +71, +60 and +34, respectively.

The contribution of the global temperature as a significant factor is further emphasized by the model runs that included only the external factors. When only the large-scale oscillations were included, the explained variance was 31 % and 49 % for the nondetrended and detrended time-series, respectively. When the global temperature was

Table 4 Summary of the significant predictors, the variance explained (R^2) and the SS derived at the six runs of the regression model, applied for the smoothed data (by 11-year time-window)

Data	Potential predictors	Significant predictors (in descending order of importance)	Variance explained (%)	SS
11-y smoothed time-series	CL, LSosci, GlobT	CL, NINO, GlobT, NAO	88	62
	LSosci, GlobT	MOI2, GlobT, NCP, EAWR, NAO	66	33
	LSosci	MOI2, NCP	31	12
Detrended 11-y smoothed time-series	CL, LSosci, GlobT	CL, NAO, MOI2, GlobT	88	71
	LSosci, GlobT	GlobT, EAWR, MOI2, NCP, NAO	83	60
	LSosci	MOI2, NCP, EAWR, NAO	49	24

The abbreviations CL, LSosci and GlobT denote occurrence of Cyprus lows, large-scale oscillations and global temperature anomaly

added, the rainfall variance explained increased considerably to 66 and 83 % for the nondetrended and detrended time-series, respectively (see Table 4).

Summary and conclusions

This study analyzes variations and trends in the rain regime of Israel, concentrating on the period 1975–2010, during which persistent global warming is observed. A major effort was devoted to study the factors explaining the rainfall variations on the inter-annual and inter-decadal time-scales, done for extended period, 1953–2010. The factors examined are the occurrence of the rain-producing synoptic systems and external factors, that is, large-scale oscillations affecting the MB and Europe and the global temperature.

The rainfall in the study region shows an increase toward the early 1990s, followed by a decrease, at a higher rate, toward the end of the study period. This decrease is also manifested by the latest seven rain seasons, being all below the long-term mean. The linear trend for the study period (1975–2010) shows a small, statistically insignificant, decrease for the region with >100 mm, at a rate of ~ 2 %/decade. The significance level of a trend depends on the inter-annual variability of the annual rainfall. Nevertheless, in spite of the larger rainfall variability in the super-arid region of Israel (over 50 %), only there the decreasing trend was found statistically significant.

In light of the expected drying over the Mediterranean region as a part of global warming (e.g., IPCC 2007), inter-annual variations and potential displacement of the aridity lines were inspected. The borders separating between the wet (Mediterranean), semi-arid and the arid climatic regions were found to propagate southward, toward the arid region, till the mid-1990s, and since then withdrew back, toward the wet region, at a larger rate, consistently with the inter-decadal rainfall variations. Based on Köppen climate classification, a rise in the annual temperature means an increase in the thresholds defining the aridity lines. This leads to the conclusion that the significant temperature increase observed over the eastern MB (e.g., Saaroni et al. 2003; Ziv et al. 2005) implies a shift of the aridity lines northward, beyond that implied by the rainfall decrease alone. The future warming predictions for this region (e.g., IPCC 2007; Lionello and Giorgi 2007; Alpert et al. 2008; Kitoh et al. 2008; Jin et al. 2010; Raible et al. 2010; Krichak et al. 2011) imply retreat of the aridity lines toward the wet region, with its related environmental implications.

The decreasing trend of the annual rainfall in the study period is contributed mainly by the spring season, in which its average rate exceeds 15 %/decade, statistically significant in most of the regions. Together with the decrease in

the autumn, it implies a shortening of the rainy season, as reflected by the period between the time by which 10 and 90 % of the annual rainfall is accumulated. The length of the rainy season shows a negative trend of ~ 4 days/decade, though statistically insignificant. The duration of rain spells does not show any trend, but the dry spells have become longer, a trend that was found statistically significant in most of the stations. This trend has an impact on ecosystems, agriculture and water management. For instance, during longer dry spells, the soil may become dryer and therefore irrigation is required, even in the middle of the rainy season.

The inter-annual fluctuations in the rainfall were found to be controlled mainly by the occurrence of the dominant regional rain-producing system, the Cyprus low (CL), with a correlation of $>+0.7$ in the wet region of Israel, in agreement with Saaroni et al. (2010a). In addition, several large-scale oscillations, the Nino3.4, EA-WR, NCP and MOI2, were found significantly correlated with the annual rainfall, but not the NAO, neither the global temperature. A simple regression model showed that the CL occurrence and the MOI2 are the controlling factors of the inter-annual rainfall variation, explaining 53 % of its variance.

The factors governing the inter-decadal rainfall variations were identified by applying the regression model on the time-series of the rainfall and the potential factors for the extended period (1953–2010), smoothed by 11-year time-window. For this time-scale, the CL occurrence was found the most significant, followed by large-scale oscillations (with different composition for the nondetrended and detrended time-series) and the global temperature, explaining together 88 % of the variance.

The external factors (the large-scale oscillations and the global temperature) were found to explain 66 and 83 % of the variance on the inter-decadal time-scale for the nondetrended and detrended time-series, respectively. The prominent inter-decadal rainfall variations, that is, the maximum in the 1990s and the minimum in the first decade of the twenty-first century, occurred when all the large-scale oscillations were in their positive and negative phases, respectively (see Fig. 8b). This is in contrast with the period between the 1950s and the 1980s where the large-scale oscillations were not in-phase.

As for the global temperature, it explains half of the variance explained by all of the external factors (see Table 4). It may be speculated that the relative downward drift of the normalized rainfall curve with respect to that of the large-scale oscillations (seen in Fig. 8b) is a manifestation of the effect of global temperature on the regional rainfall, particularly the warming trend from the mid-1970s onward. The negative sign of the coefficient of the global temperature in the regression model supports the expected rainfall decrease in the study region under global warming.

The general decreasing trend in the rainfall over the study region, and the finding that this decrease is statistically significant over its southern part, may be regarded as a manifestation of the increased influence of the subtropical high over the MB. Such an evolution is implied by an expansion of the Hadley cell, attributed to the global warming (Seidel et al. 2008). This influence is expected to be pronounced when the Mediterranean cyclone track retreats northward, that is, in dry spells and in the transition seasons. The shortening of the rainy season, though statistically insignificant, and the lengthening of the dry spells, found in this study, may therefore be regarded as first signs of the subtropical high enhancement over the MB. This process is expected to be most pronounced in the study region since it is a part of the southern edge of the MB. In light of the climate models prediction for future decrease in Mediterranean cyclones (e.g., Lionello and Giorgi 2007; Raible et al. 2010), our findings, reflecting general drying, should be taken as a first alarm for this vulnerable region even though most of them are still statistically insignificant.

The high inter-annual rainfall variability over the study region implies that the probability to identify statistically significant trends within short periods, such as this study period, is rather low. Morin (2011) showed that if a trend of 25 mm/decade ($\sim 3\%$ /decade, close to that found for the study period) would take place at north Israel during 50 years, its probability to be statistically significant is rather low. Since such a trend has far-reaching environmental implications, ignoring it may reject any discussion of decision makers on potential solutions. However, continual study of variations and trends in the rainfall regime, and its controlling factors, is essential for the MB as a whole, and its eastern part in particular.

Acknowledgments The authors thank the Ministry of Environmental Protection (grant number 8-810) and the Israeli Science Foundation (ISF, grant number 108/10) that funded this study. Special thanks are due to the climatology department in the Israeli Meteorology Services that cooperated in conducting this research and specifically to Dr. Noam Halfon who did the GIS maps, Mr. Avner Forshpan and Dr. Isabella Osetinski-Tzidki. We wish also to thank Mrs. Ronit Sagi for her contribution to the statistical analysis.

References

- Alpert P, Neeman BU, Shay-El Y (1990) Climatological analysis of Mediterranean cyclones using ECMWF data. *Tellus* 42A:65–77
- Alpert P, Ben-Gai T, Baharad A, Benjamini Y, Yekutieli D, Colacino M, Diodato L, Ramis C, Homar V, Romero R, Michaelides S, Manes A (2002) Evidence for increase of extreme daily rainfall in the Mediterranean in spite of Decrease in Total Values. *Geophys Res Lett* 29(1536):31–34. doi:10.1029/2001GL013554
- Alpert P, Osetinsky I, Ziv B, Shafir H (2004) Semi-objective classification for daily synoptic systems: application to the eastern Mediterranean climate change. *Int J Climatol* 24(8):1001–1011
- Alpert P, Krichak SO, Shafir H, Haim D, Osetinsky I (2008) Climatic trends to extremes employing regional modeling and statistical interpretation over the E. Mediterranean. *Global and Planetary Change* 63:163–170
- Ben-Gai T, Bitan A, Manes A, Alpert P (1994) Long-term changes in annual rainfall patterns in southern Israel. *Theor Appl Climatol* 49:59–67
- Ben-Gai T, Bitan A, Manes A, Alpert P, Rubin S (1998) Spatial and temporal changes in annual rainfall frequency distribution patterns in Israel. *Theor Appl Climatol* 61:177–190
- Branston AG, Livezey RE (1987) Classification, seasonality and persistence of low-frequency atmospheric circulation patterns. *Mon Wea Rev* 115:1083–1126
- Conté M, Giuffrida A, Tedesco S (1989) The Mediterranean Oscillation: impact on precipitation and hydrology in Italy. In: Conference on Climate and Water Publications of the Academy of Finland 9/89, 1:121–137
- Dayan U, Sharon D (1980) Meteorological parameters for discriminating between widespread and spotty storms in the Negev. *Isr J Earth Sci* 29(4):253–256
- Dayan U, Ziv B, Margalit A, Morin E, Sharon D (2001) A severe autumn storm over the middle-east: synoptic and mesoscale convection analysis. *Theor Appl Clim* 69:103–122
- ESRI Inc (2008) ArcMap™ 9.3. Environmental Systems Research Institute Inc, Redlands, CA
- Goldreich Y (2003) The Climate of Israel: Observation, Research and Application. Kluwer Academic Publishes, New York, USA
- Helsel DR, Hirsch RM (2002) Statistical Methods in Water Resources Techniques of Water Resources Investigations, Book 4, chapter A3. U.S. Geological Survey, 522 p
- IPCC Intergovernmental Panel on Climate Change (2007) The Physical Science Basis, Summary for Policymakers (contribution of WG I to the 4th Assessment Report of the IPCC), Cambridge and New York: Cambridge University Press. <http://ipcc-wg1.ucar.edu/>
- Jacobeit J (1987) Variations of trough positions and precipitation patterns in the Mediterranean area. *Int J Climatol* 7:453–476
- Jin F, Kitoh A, Alpert P (2010) Water cycle changes over the Mediterranean: a comparison study of a super-high-resolution global model with CMIP3. *Phil Trans Roy Soc A* 368:1–13
- Kahana R, Ziv B, Enzel Y, Dayan U (2002) Synoptic climatology of major floods in the Negev desert, Israel. *Int J Climatol* 22: 867–882
- Kitoh A, Yatagai A, Alpert P (2008) First super-high-resolution model projection that the ancient “Fertile Crescent” will disappear in this century. *Hydrolo Res Lett* 2:1–4. doi:10.3178/HRL.2.1
- Kostopoulou E, Jones PD (2005) Assessment of climate extremes in the Eastern Mediterranean. *Meteor Atmos Phys* 89:69–85
- Krichak SO, Alpert P (2005) Decadal trends in the East Atlantic–West Russia pattern and Mediterranean precipitation. *Int J Climatol* 25:183–192
- Krichak SO, Kishcha P, Alpert P (2002) Decadal trends of main Eurasian oscillations and the Mediterranean precipitation. *Theor Appl Climatol* 72:209–220
- Krichak SO, Breitgand JS, Samuels R, Alpert P (2011) A double-resolution transient RCM climate change simulation experiment for near-coastal eastern zone of the Eastern Mediterranean region. *Theor Appl Climatol* 103:167–195
- Kutiel H, Benaroch Y (2002) North Sea–Caspian pattern (NCP)—an upper level atmospheric teleconnection affecting the eastern Mediterranean: identification and definition. *Theor Appl Climatol* 71:17–28
- Kutiel H, Paz S (1998) Sea level pressure departures in the Mediterranean and their relationship with monthly rainfall conditions in Israel. *Theor Appl Climatol* 60:93–109

- Lionello P, Giorgi F (2007) Winter precipitation and cyclones in the Mediterranean region: future climate scenarios in a regional simulation. *Adv GeoSci* 12:153–158
- McKnight TL, Hess D (2008) *Physical Geography: A Landscape Appreciation*. 9th edition, Prentice Hall, 720 p
- Morin E (2011) To know what we cannot know: global mapping of minimal detectable absolute trends in annual precipitation. *Water Resour Res* 47:W07505. doi:[10.1029/2010WR009798](https://doi.org/10.1029/2010WR009798)
- Paz S, Kutiel H (2003) Rainfall regime uncertainty (RRU) in an eastern Mediterranean region—a methodological approach. *Isr J Earth Sci* 52:47–63
- Perlin N, Alpert P (2001) Effects of land-use modification on potential increase of convection—a numerical study in south Israel. *J Geophys Res* 106:22,621–22,634
- Price C, Stone L, Huppert A, Rajagopalan B, Alpert P (1998) A possible link between El-Nino and precipitation in Israel. *Geophys Res Lett* 25(21):3963–3966
- Raible CC, Ziv B, Saaroni H, Wild M (2010) Winter synoptic-scale variability over the Mediterranean Basin under future climate conditions as simulated by the ECHAM5. *Clim Dyn* 35(2–3):473–488
- Reiser H, Kutiel H (2009) Rainfall uncertainty in the Mediterranean: definitions of the daily rainfall threshold (DRT) and the rainy season length (RSL). *Theor Appl Climatol* 97:151–162
- Saaroni H, Ziv B, Edelson J, Alpert P (2003) Long-term variations in summer temperatures over the Eastern Mediterranean. *Geophys Res Lett* 30(18):1946. doi:[10.1029/2003GLO17742](https://doi.org/10.1029/2003GLO17742)
- Saaroni H, Halfon H, Ziv B, Alpert P, Kutiel H (2010a) Links between the rainfall regime in Israel and location and intensity of Cyprus Lows. *Int J Climatol* 30:1014–1025. doi:[10.1002/joc.1912](https://doi.org/10.1002/joc.1912)
- Saaroni H, Ziv B, Uman T (2010b) Does a synoptic classification indicate the NO_x pollution potential? The case of the metropolitan area of Tel Aviv, Israel. *Water Air Soil Pollut* 207(1–4):139–155. doi:[10.1007/s11270-009-0125-6](https://doi.org/10.1007/s11270-009-0125-6)
- Seidel DJ, Fu Q, Randel WJ, Reichler TJ (2008) Widening of the tropical belt in a changing climate. *Nat Geosci* 1:21–24
- Shay-El Y, Alpert P (1991) A diagnostic study of winter diabatic heating in the Mediterranean in relation with cyclones. *Quart J R Meteor Soc* 117:715–747
- Shlomi Y, Ginat H (2009) Rainfall in the Arava 1950–2008, Preliminary report. Scientific report submitted to the water and the Arava drainage authorities, Dead Sea and Arava Science Center, 23 p. (in Hebrew)
- Sousa PM, Trigo RM, Aizpurua P, Nieto R, Gimeno L, Garcia-Herrera R (2011) Trends and extremes of drought indices throughout the 20th century in the Mediterranean. *Nat Hazards Earth Syst Sci* 11:33–51. doi:[10.5194/nhess-11-33-2011](https://doi.org/10.5194/nhess-11-33-2011)
- Toreti A, Xoplaki E, Maraun D, Kuglitsch FG, Wanner H, Luterbacher J (2010) Characterization of extreme winter precipitation in Mediterranean coastal sites and associated anomalous atmospheric circulation patterns. *Nat Hazards Earth Syst Sci* 10:1037–1050
- Tsvieli Y, Zangvil A (2005) Synoptic climatological analysis of “wet” and “dry” Red Sea Troughs over Israel. *Int J Climatol* 25:1997–2015
- Wilks DS (2011) *Statistical methods in the Atmospheric Sciences* (3rd ed.), Elsevier, Amsterdam
- Xoplaki E, Gonz'alez-Rouco JF, Luterbacher J, Wanner H (2004) Wet season Mediterranean precipitation variability: influence of large-scale dynamics and trends. *Clim Dyn* 23:63–78
- Yosef Y, Saaroni H, Alpert P (2009) Trends in daily rainfall intensity over Israel 1950/1–2003/4. *The Open Atmos Sci J* 3:196–203
- Zangvil A, Karas S, Sasson A (2003) Connection between Eastern Mediterranean seasonal mean 500-hPa height and sea-level pressure pattern and the spatial rainfall distribution over Israel. *Int J Climatol* 23:1567–1576
- Zhang X, Aguilar E, Sensoy S et al (2005) Trends in Middle East climate extreme indices from 1950 to 2003. *J Geophys Res* 110:D22104
- Ziv B, Saaroni H, Baharad A, Yekutieli D, Alpert P (2005) Indications for aggravation in summer heat conditions over the Mediterranean Basin. *Geophys Res Lett* 32(12):L12706
- Ziv B, Dayan U, Kushnir Y, Roth C, Enzel Y (2006) Regional and global atmospheric patterns governing rainfall in the southern Levant. *Int J Climatol* 26:55–73